

Fast impression painting using multi-color fused deposition modeling with a diamond hotend

Riccardo Tonello^{1,2}, Fereshteh Abedini³, David Bue Pedersen² and Jeppe Revall Frisvad¹

¹ Department of Computer Science, Technical University of Denmark, Building 324, R. Petersens Pl., 2800 Kgs. Lyngby, Denmark

² Department of Mechanical Engineering, Technical University of Denmark, Building 427A, Produktionstorvet, 2800 Kgs. Lyngby, Denmark

³ Department of Science and Technology, Linköping University, Kopparhammaren 2, KO2038, Campus Norrköping, Sweden

INTRODUCTION

Fused deposition modeling (FDM) is an easily accessible technology for additive manufacturing. The use of a diamond hotend [1] is one way to get multiple colors in FDM. This is a flexible and versatile approach that combines multiple colorful filaments in one outend. The diamond hotend thus offers multi-color printing with the simplicity of a single extrusion 3D printer.

The color gamut (set of printable colors) provided by a multiple-in-one-out printer is determined by its blending of different filaments in the nozzle tip. A drawback of this system is the transition time that the printer requires to be able to switch completely the print color. This can lead to non-uniform print areas with undesired colors.

Another problem is the accuracy of the details. The system works with multiple extrusion drivers and slight differences in their feeding forces might incur uncontrolled gradients of pressures that result in printing artifacts. This can generate halftone hatches that are not overall consistent, and oozing of the nozzle tip often happens in undesired areas when the extrusion is stopped, despite the use of a filament retraction length.

The traditional method used to overcome these problems and exhaust the nozzle before printing a new color is the purge tower. However, this strategy increases the overall printing time and the waste of material. Moreover, when multiple colors are used to print the same layer, the size of the purge tower might become bigger than the printed area. The reason is that the purge tower receives the length of the previous filament stuck between the mixing chamber and the nozzle tip. It also receives the length of the next filament that

mixes with the previous one, which is pulled out while being unset.

Our goal is to avoid the purge tower in order to improve speed and reduce waste in this type of multi-color FDM printing. This requires a different workflow. Our idea is to control the number of steps before switching to the next color and the length and time of the retraction of the filament when foreseeing movement without extrusion. However, increasing the speed worsens the accuracy and viceversa [2], so we focus on fast printing of impression paintings, where the accuracy is not an essential factor.

In addition, we want to corroborate these strategies with a supportive visualization tool that can process images, reorganize them according to the available color gamut of the printer and detect the number of points that we need on the buildplate for a given print job. We test our multi-color method by printing an impression painting corresponding to a given input image.

RELATED WORK

Rather few multi-color FDM technologies are currently available on the market. Dual extruder 3D printers [3, 4], filament splicing tools [5, 6], full color 3D printers [7], and mixed color 3D printers [8] are the only ones able to provide a wider range of colors in a print.

The diamond hotend is the main technology in the field of mixed color 3D printing. It consists of several inlets where the filaments blend and only

one outlet (multiple-in-one-out nozzle). In previous work, Song et al. [8] focused on production of color gradients with the use of translucent filaments deposited in thin strata. They also showed some lithophanes of images exploiting such techniques. However, in their work, purge towers were used to clean the nozzle tip before changing color. Furthermore, a lithophane is a 3D image given by superposition of layers according to a topographic model, and with multicolor buildsets, it can be fabricated only with the use of translucent filaments. In our work, we rely neither on translucent filaments nor on the use of purge towers.

Without purge towers, oozing is a relevant and constant factor that must be considered. In fact, when the nozzle stops the print and moves to a different position, if the toolhead lifts to avoid intersecting other already printed parts, the pressure gradient given by the melt conformation and the gap between the buildplate and the nozzle tip occupied by the melt itself causes the filament to flow down and bleed on all areas along the movement made [9, 10].

A related work is from Hergel and Lefebvre [3], who designed optimal algorithms to reduce oozing. Their idea is a toolpath planner that avoids formerly printed parts. This is useful for limiting the ooze, but when the part to reproduce is a painting, such strategies are often not helpful because while filling the buildplate with masks of different colors, safe areas to move the extruder to, without moving over printed parts, are fewer and fewer.

In order to fight the oozing effect, we maximize the retraction length and increase the speed of the extruder when it moves without extruding filament material.

EXPERIMENTAL PART

Workflow and methods

To demonstrate our method, we designed a tool for computing and visualizing the needed G-code (geometric code used for control of the FDM printer). This consists of:

- Color threshold based segmentation of a given image. We choose a number of print colors (six in our demonstration) and reorder the segments in color clusters according to the available gamut of the printer.
- Removal of small areas of pixels in order to facilitate the printing operations.
- Creation of the G-code, consistent with the fastest color transition and the best strategies



FIGURE 1: Color threshold based segmentation with superpixels in order to remove spare pixels.

to reduce the oozing effect and avoid extrusion movements of the tool head.

- Calibration of the printing parameters.

In the first part, we took advantage of superpixels and clustering techniques. Because we restricted the printer's gamut to six colors, we employed k -means clustering [11] to partition the image into six clusters (i.e., $k = 6$). We used superpixels to avoid the rigid structure of the pixels and detached single pixels in clusters.

Superpixel algorithms group pixels into regions with similar perceptual properties that adhere well to the image edges. There are many methods for generating superpixels. However, the simple linear iterative clustering (SLIC) algorithm has proven a good choice [12]. Thus, we employed the SLIC algorithm to group pixels with similar values in the CIELAB color space into superpixels.

Use of superpixels improves the segmentation performance by reducing its complexity. For instance, if our target image (FIG. 1, left) is of resolution 250×187 , SLIC can reduce the number of picture elements from 46750 pixels to 2028 superpixels.

In addition, superpixels provide more information than regular pixels. So, to further improve the segmentation, we supplemented the segmentation algorithm with the mean value of each superpixel. As a result, the k -means clustering algorithm prefers grouping superpixels with similar mean CIELAB values into the same cluster. FIG. 1 (right) shows the result of using superpixels and k -means clustering techniques to segment the image into 6 clusters.

After producing the segmented image, we created an operational dataset of filament mixing ratios sorted by the minimum color space distance between the colors in the printer gamut. This sorting enables us to minimize the color

transition between different hues during a print, which is otherwise the constraint of multi-color FDM that leads to use of purge towers.

We can then abandon the use of purge towers and reduce the presence of artifacts and ooze through a smaller stepwise transition between colors during printing. However, these two improvements are inversely proportional, since the absence of an exhaust tower and the faster printing are sources for artifacts and decrease the overall accuracy.

To find a good tradeoff, we developed a customized G-code following two different approaches. Obtaining masks for each color given by the segmentation of the processed image, the first method consisted of detecting and storing all the points of the borders (light blue pixels in FIG. 2). After this, we excluded all the identified border points and repeated the previous step, with the only difference that we did not store the points this time (yellow pixels in FIG.2). Alternating a border with stored points and one without stored points, it was possible to create a concentric toolpath [FIG. 2].

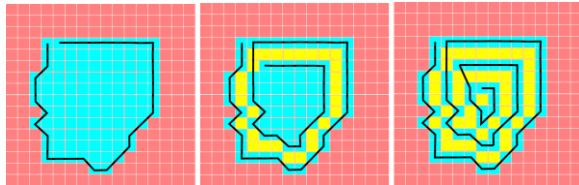


FIGURE 2: Toolpath generation with contour detection.

Another approach is to define two filter grids, respectively 3x3 and 5x5 in order to have an idea of the neighbourhood of the detected pixel. This method enables a higher freedom to operate and in this way, it has been possible to define strategies that avoid singularities such as non-Euclidean geometries, which may incur overlapping of printed filament or too narrow print areas.

For this approach, we devised the following G-code generation strategy (FIG. 3):

- Use of a preferred print direction (v) with clockwise ordering (numbers in FIG. 3A). We have a preferred direction along a coordinate axis ($v \in [1,3,5,7]$). When selecting extrusion direction, we try directions $v-1, v, v+1$ (with this priority). If the pixels in these three directions are all unavailable, we shift our preferred direction 90° clockwise, $v := (v + 1 \bmod 8) + 1$ (FIG. 3B), and we continue.

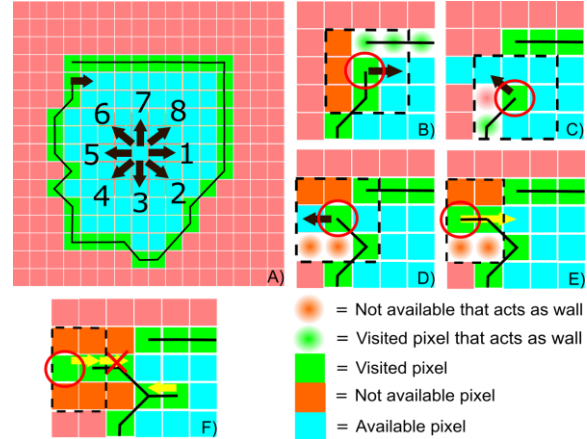


FIGURE 3: Strategies adopted to define a concentric toolpath.

- If we reach a dead-end (FIG. 3E), the tool-head goes back a few steps without extruding and selects a new direction as before.
- If we move back for a maximum number of steps without finding a new direction, the toolpath breaks, and we continue from the next unvisited point in the image (FIG. 3F).
- Selecting a 5x5 grid, additional features are added to prevent that the toolpath breaks (FIG. 3B-C-D-E).

After designing the G-code tool path, we implemented a supportive visualization tool (FIG. 4) in order to understand if all points were correctly transcribed and the fastest transition between colors was respected.

The black spots in FIG. 4 are excluded points. These are points without extrusion or print areas too small to be meaningfully printed. We inspected the outputs of our different approaches using a commercial G-code viewer [13], an example is in FIG. 5.

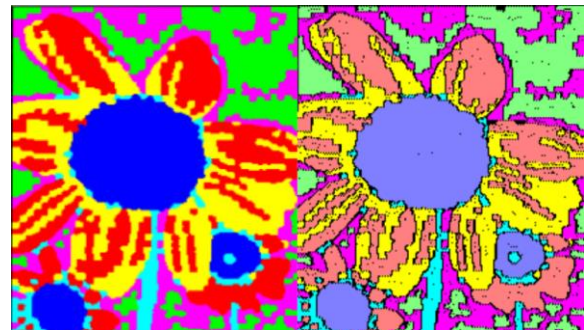


FIGURE 4: Visualization tool (right image) with points of extrusion.

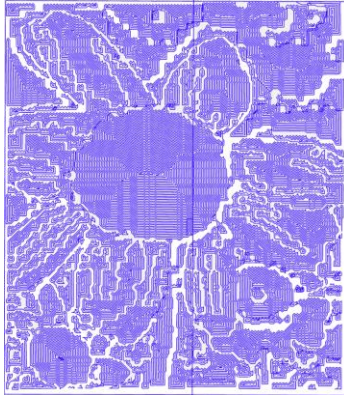


FIGURE 5: G-code viewer [13].

Experiments

After creating the G-code file, we tested it on a diamond hotend 3D printer. With the aim of reducing the ooze and creating some fast prints without a purge tower, we calibrated the printer accordingly. To reduce the oozing effect, we predicted the amount of visible material dropped and dragged by the extruder across the buildplate after stopping the printing and computed the number of points in advance to start retracting the filament. We used trial and error until we reached a promising result for the square with concentric infill.

We used a very similar approach when switching colors. By computing the length of filament needed for the color transition, we inserted the switch to another color a number of points before completing the section, so as to reduce the color transition to the center and the border of each printing area. We tackled the experiments by designing a simple version of a painting: a set of squares next to each other to prove the concept. The extruder prints at 220 °C with 15 points of retraction length for each no extrusion movement, while it counts 15 points ahead to switch to Cyan, Magenta and Yellow, but 35 points for the combinations of them, since higher pressures are needed to effectively extrude 2 filaments at the same time. We printed three layers in our tests because the result with one layer became too brittle to be detached from the buildplate without breaking.



FIGURE 6: G-code points of six squares in the visualization tool (top). Six 3D printed squares without purge tower (bottom).

CONCLUSIONS

Even though some simple geometries can be printed without the use of the purge tower and with few precautions in terms of retraction length, more complex geometries are still hard to print without some additional aids. However, it is possible to print fast impressions as shown in the figure below and we are confident that it is ultimately possible to improve the accuracy.



FIGURE 7: Image, processed image, and 3D printed image.

ACKNOWLEDGMENT

This project was funded by ApPEARS (Appearance Printing European Advanced Research School), the European Union's Horizon 2020 programme under the Marie Skłodowska Curie grant agreement No.814158

REFERENCES

- [1] A. Bowyer, "Diamond Hotend," 2018. [Online]. Available: https://reprap.org/wiki/Diamond_Hotend.
- [2] L. Levinskas, "Research of dimensional accuracy and surface quality dependency on printing speed of FDM 3D printed parts," MSc thesis, Kaunas University of Technology, Kaunas, 2019.
- [3] J. Hergel and S. Lefebvre, "Clean color: Improving multi-filament 3D prints," *Computer Graphics Forum*, vol. 33, no. 2, pp. 469-478, 2014.
- [4] O. A. Mohamed, S. H. Masood and J. L. Bhowmik, "Optimization of fused deposition modeling process parameters," *Advances in Manufacturing*, vol. 3, pp. 42-53, 2015.
- [5] H. Takahashi, P. Punpongsanon and J. Kim, "Programmable Filament: Printed Filaments for Multi-Material 3D Printing," in *ACM Symposium on User Interface Software and Technology (UIST)*, 2020.
- [6] Mosaic, "Mosaic Palette," Mosaic, 2015. [Online]. Available: <https://www.mosaicmfg.com/products/palette-3-pro>.
- [7] XYZPrinting, "Ces 2020 Innovation Award Product," XYZPrinting, 2020. [Online]. Available: <https://www.ces.tech/Innovation-Awards/Honorees/2020/Honorees/D/davinci-color-5D.aspx>.
- [8] H. Song, J. Martínez, P. Bedell, N. Vennin and S. Lefebvre, "Colored fused filament fabrication," *ACM Transactions on Graphics*, vol. 38, no. 5, pp. 141:1-141:11, 2019.
- [9] M. E. Mackay, Z. R. Swain and C. R. Banbury, "The performance of the hot end in a plasticating 3D printer," *Journal of Rheology*, vol. 61, pp. 229-236, 2017.
- [10] R. Comminal, M. P. Serdeczny, D. B. Pedersen and J. Spangenberg, "Numerical modeling of the strand deposition flow in extrusion-based additive manufacturing," *Additive Manufacturing*, vol. 20, pp. 68-76, 2018.
- [11] J. MacQuenn, "Some methods for classification and analysis of multivariate observations," *Fifth Berkeley Symposium on Mathematical Statistics and Probability*, vol. 1, pp. 281-297, 1967.
- [12] R. Achanta, A. Shaji, K. Smith, A. Lucchi, P. Fua and S. Süsstrunk, "SLIC Superpixels Compared to State-of-the-Art," *IEEE Transactions on Pattern Analysis and Machine Intelligence*, vol. 34, no. 11, pp. 2274-2282, 2012.
- [13] L. Xander, "NC Viewer V1.1.3," NC Viewer, 2018. [Online]. Available: <https://ncviewer.com/>.